Open Access

Recent Progress in Materials

LIDSEN Publishing Inc.

Original Research

Role of Point of Zero Charge in the Adsorption of Cationic Textile Dye on Standard Biochars from Aqueous Solutions: Selection Criteria and Performance Assessment

Sabine Neusatz Guilhen [1, *], Tamires Watanabe [1], Thalita Tieko Silva [1], Suzimara Rovani [2], Júlio Takehiro Marumo [1], Jorge Alberto Soares Tenório [2], Ondřej Mašek [3], Leandro Goulart de Araujo [1, ‡]

1. Instituto de Pesquisas Energéticas e Nucleares (IPEN-CNEN/SP) - Av. Prof. Lineu Prestes, 2242, Cidade Universitária, 05508-000, São Paulo, SP, Brazil; E-Mails: snguilhen@ipen.br; tamireswatanabe@gmail.com; thalitatieko@gmail.com; jtmarumo@ipen.br; lgoulart@alumni.usp.br
2. Escola Politécnica, Universidade de São Paulo - Rua do Lago, 250, Cidade Universitária, 05508-080 - São Paulo, SP, Brazil; E-Mails: suzirovani@gmail.com; jtenorio@usp.br
3. UK Biochar Research Centre, University of Edinburgh, School of Geosciences, Crew Building, Alexander Crum Brown Road, EH9 3FF, Edinburgh, UK; E-Mail: ondrej.masek@ed.ac.uk

‡ Current Affiliation: Institut Jean Lamour, CNRS UMR7198, Université de Lorraine, Ecole Nationale Supérieure des Technologies et Industries du Bois (ENSTIB), 27 Rue Philippe Séguin, BP 1041, 88051 Epinal Cedex 9, France

* **Correspondence:** Sabine Neusatz Guilhen; E-Mail: snguilhen@ipen.br

Academic Editor: Mattia Bartoli

Special Issue: Biochar Based Composite Materials

Recent Progress in Materials
2022, volume 4, issue 2
doi:10.21926/rpm.2202010

Received: April 19, 2022
Accepted: May 07, 2022
Published: May 19, 2022

Abstract

The point of zero charge (PZC) is an inherent electrokinetic property of biochars (BC). It influences the adsorption process under certain pH conditions. Herein, we report the method of determination of the PZC values of ten standard BCs. We used the salt addition method to select the BCs with suitable properties for methylene blue (MB) removal from

aqueous solutions. The standard BCs were obtained by pyrolyzing five different biomasses at two distinct temperatures (550°C and 700°C). The BCs derived from rice husk (pH_{PZC} at 7.22 and 7.64 for RH550 and RH700, respectively) and softwood pellets (pH_{PZC} at 6.57 and 6.78 for SWP500 and SWP700, respectively) were selected for their compatibility with cationic dyes such as MB. Results from adsorption experiments indicated the potential use of the RH biochar as an adsorbent for the removal of MB from aqueous solutions. The removal efficiencies were 68.83% and 71.97% for RH550 and RH700, respectively. Considerably low values were obtained for SWP550 and SWP700 (21.61% and 22.84%, respectively). Equilibrium was achieved at 2 h for RH550 and 1 h for RH700, and the adsorption kinetics for the RH BCs could be described by a pseudo-second order equation. The results revealed that even when produced under comparable conditions, BCs obtained from different feedstocks exhibited different cationic dye removing abilities. BCs optimized for the removal of cationic or anionic dyes can be easily engineered by appropriately matching the feedstock with the processing conditions.

Keywords
Adsorption; biochar; cationic dye; methylene blue; point of zero charge; salt addition

1. Introduction

Textile manufacturing processes cause water pollution, which is of serious concern worldwide. Due to their toxic nature, synthetic dyes can severely impact the environment when untreated or partially treated effluents are discharged into water bodies. Textile dyes not only compromise the aesthetic quality of water but also negatively influence the process of photosynthesis, inhibiting plant growth. Thus, it also affects the health of aquatic biota [1]. Generally, a large percentage of the dye does not bind to the fabric during the coloration process. The unbound dye - approximately 10 to 15% - is released into the wastewater stream [2-8]. The synthetic dyes in water exert adverse effects on many forms of life, and this can be attributed to the toxicity, mutagenicity, and/or carcinogenicity of their components and by-products [9].

Dyes can be classified as (1) anionic dyes, which are divided into direct, acid, and reactive dyes; (2) nonionic dyes, which are also known as disperse dyes; and (3) cationic dyes, which comprise of all basic dyes [10]. Methylene blue (MB) is a well-known thiazine cationic dye which is widely used in the leather, ceramics, and textile industries [11, 12]. Decolorization processes are conducted to treat wastewater before dye-containing wastewaters are released into the water streams. This is because most dyes, including MB, are resistant to chemical and biological treatment methods. During the process of decomposition of dyes, substances that are more toxic than the dyes may be produced [13].

Various methods have been reported over the years for the removal of toxic dyes [14, 15]. These methods include aqueous removal methods such as biological, coagulation, coagulation-flocculation, oxidation, ozonation, and adsorption. The adsorption method is a very simple and effective process that is widely used for the removal of dyes from wastewater [16, 17].

Many different adsorbents (such as zeolites, resins, clay minerals, and activated carbons) can be used for wastewater treatment and purification [18-21]. BCs are receiving increasing attention as potential adsorbent materials. This is because they are characterized by a porous structure, contain a charged surface, and consist of numerous surface functional groups. Several studies have demonstrated that BCs can be used as low-cost adsorbents for the treatment of aqueous solutions contaminated with dyes [22-27].

BCs are obtained through thermal degradation of carbon-rich biomass in the presence of little or no oxygen [28]. Not only is there a multitude of biomasses available to produce BC, but they are also considered to be natural and renewable sources that are present in abundance. There are a number of biomasses that can be used as feedstock for BC, including rice straw, rice husk, bamboo, corn stover, peanut shells, softwood, etc.

The point of zero charge (PZC) is an electrokinetic property of materials, such as fibers. The determination of PZC is critical for the dyeing processes as it influences the adsorption of dyes used during the dyeing of fibers [29]. During the process of dyeing, the ionic charge of the protein fibers is affected by the pH of the bath in which the fibers are immersed. Similarly, pH is also important in the case of BC as an adsorbent, given that the process of dye adsorption will depend on not only the PZC of the BC but also the pH of the dye solution.

At the pH corresponding to the PZC (pH_{PZC}), the net surface charge is zero, and the diffuse ion swarm vanishes. In other words, under these conditions, the BC has a neutral charge. It is also called the isoelectric point (IEP), as at this pH value, the particles do not move when exposed to an electric field [30]. At pH_{PZC}, equal amounts of positive and negative charges are present. Thus, it is faulty to state that the surface is devoid of charge [31].

The determination of PZC can help optimize the process of selection of a BC that can be used as an adsorbent for the removal of MB from aqueous solutions. Adsorbents with low PZC values are compatible with cationic dyes, such as MB, whereas adsorbents with high PZC values are more suitable for the capture of anionic dyes.

This study describes the method of determination of the PZC of ten standard BCs, developed and provided by the UK Biochar Research Centre (UKBRC). The results have been compared, and the salt addition method was used for the studies. It was possible to compare the results as these BCs were produced under standard conditions. Pyrolytic temperature, residence time, type of raw material, and thermochemical conversion technology significantly affect the properties of BCs and, consequently, affect the applicability of the BCs as adsorbents [32]. The ten standard BCs were obtained by pyrolyzing the raw materials at similar temperatures and residence times. The differences in the properties of the BCs arise from the use of different feedstocks. Under the same pyrolysis conditions, the adsorption capacity of BCs varies based on the raw material sources. The differences can be attributed to the mineral components (such as CO_3^{2-} and PO_4^{3-}) present in the systems [33-36]. The information on PZC can be used for selecting suitable BCs for the efficient removal of MB and other dyes from aqueous solutions.

The determination of the PZC values of the standard BCs provided by the UKBRC has not been previously addressed. Furthermore, to the best of our knowledge, these materials have not been previously investigated by varying the adsorbent dosages and under conditions of different pyrolytic temperatures for the adsorption of MB. The removal efficiency (R) for MB and the adsorption capacity (q) were calculated under specified conditions for the BCs selected. The experiments were based on the PZC data. Furthermore, the morphology of each standard BC was

investigated using the scanning electron microscopy (SEM) technique. The surface properties of the selected BCs were analyzed using the Fourier-Transform infrared spectroscopy (FTIR) technique. Finally, non-linear kinetic models were outlined to predict the MB adsorption kinetics on the selected BCs.

2. Materials and Methods

2.1 Reagents and Solutions

Solutions of $^{-}NaNO_3$ (0.1 mol L^{-1}) were used to maintain the ionic strength during the experiments. Standardized solutions of $^{-}HNO_3$ and NaOH (0.1 and 0.5 mol L^{-1}, respectively) were prepared for pH adjustment. All reagents were supplied by Merck (Darmstadt, HE, Germany). The solutions were prepared using ultrapure water of 18.2 MΩ cm resistivity (Barnstead Thermolyne, Iowa, USA).

2.2 BC samples

Ten different standard BCs were prepared following the process of slow pyrolysis at UKBRC (The University of Edinburgh, UK) using a pilot-scale rotary kiln pyrolysis unit. The ten BCs were obtained from a set of 5 different biomasses (rice husk, oilseed rape straw, wheat straw, miscanthus straw, and soft wood). The samples were prepared at 2 different temperatures (Table 1; 550 and 700°C; heating rate: 80°C min^{-1}; residence time: 15 min). The basic properties of each standard BC are presented in Table S1. The details were provided in the specification sheets from the UKBRC. All ten BC samples and the respective feedstocks are presented in Figure S1.

Table 1 Standard BCs furnished by UKBRC.

Biomass	**Pyrolytic Temperature**	
	550°C	**700°C**
Rice Husk	RH550	RH700
Oil Seed Rape Straw Pellets	OSR550	OSR700
Wheat Straw Pellets	WSP550	WSP700
Miscanthus Straw Pellets	MSP550	MSP700
Soft Wood Pellets	SWP550	SWP700

2.3 Preparation of the Samples

The standard BCs were ground in a cutting mill and passed over a 120-mesh screen. The fraction corresponding to particles smaller than 250 µm was selected. The selection was based on exploratory tests, and a 60-mesh sieve was used. The samples were stored in air-sealed polypropylene flasks obtained from SCP Science (Baie-D'Urfé, QC, Canada).

2.4 Determination of the PZC values

The initial pH values (pH_i) were adjusted in the range of 3-13 using NaOH and HNO_3 solutions. All experiments were performed in triplicate (biochar dosage: 10 g L^{-1}) in a $^{-}$solution of $NaNO_3$ (0.1

mol L^{-1}). The final pH values (pH_f) were recorded for the remaining suspensions after shaking the solutions for 24 h at 120 rpm.

2.5 Calibration Curve for MB

The quantitative determination of MB was performed using the ultraviolet-visible (UV-vis) spectroscopy technique using a Pharmacia Biotech Ultrospec 3000 UV/Visible spectrophotometer (Uppsala, Sweden). The absorption spectra were recorded by measuring the absorbance at 668 nm (λ_{max} = 668 nm). This wavelength corresponded to the maximum absorption of MB in the UV-vis range. The calibration curve for MB was generated to evaluate the linearity in the range considered in this study. MB solutions of different concentrations (range: 0-20 mg L^{-1}; nine points: 0, 0.05, 0.5, 1, 2.5, 5, 10, 15, and 20 mg L^{-1}) were prepared and the absorbance was recorded using the UV-vis spectrophotometer.

2.6 Sorption Experiments

Exploratory laboratory experimentation allowed the selection of the specific conditions associated with the parameters of interest. The experiments were conducted in triplicate using a solution of $^{-}$MB (initial concentration: 50 mg L^{-1}) prepared at pH 8 to evaluate the MB adsorption capacity of the BCs selected based on the PZC experiments (RH550, RH 700, SWP550, and SWP700). This solution was placed in contact with each BC (dosage: 10 g L^{-1}) and shaken for 24 h at 120 rpm. The BCs were air-dried at 110°C in a drying oven prior to conducting the experiments.

At the end of the shaking step, the supernatant was separated from the BC under conditions of centrifugation at 6,000 rpm (time: 15 min), and the MB concentration in the remaining solution was determined using UV-vis spectroscopy technique. Filtration (instead of centrifugation) was also considered to conduct this step as the residual, non-adsorbed MB in the solution could be partially retained in the filter paper. This could increase the final removal efficiency by synergistically complementing the adsorption process. This alternative was considered because many researchers studying the dye removal process by adsorption [37-42] used the filtration method to separate the adsorbent from the remaining solution. The adsorbent was alternatively separated following the filtration process, instead of centrifugation, using a medium grade double-ring quantitative filter (GE Healthcare, Chicago, IL, USA) to quantify the effect.

The extraction efficiency, R (%), was determined using the following equation:

$$R(\%) = 100 \times \left[\frac{(C_0 - C_t)}{C_0}\right], \quad (1)$$

where R is the efficiency of extraction or retention percentage, C_0 (mg L^{-1}) is the initial concentration of MB, and C_t (mg L^{-1}) represents the concentration of MB at time t.

The adsorption of MB was evaluated as a function of the adsorbent dose, pH, contact time, and initial concentration. The adsorption capacity (mg g^{-1}) of the adsorbent was calculated using Eq. (2) as follows:

$$q_t = \frac{(C_0 - C_t) \times V}{M}, \quad (2)$$

where q_t is the amount of adsorbate adsorbed per gram of the adsorbent at any time t, C_0 and C_t are the concentrations of the adsorbate in the initial solution and at time t, respectively (mg L^{-1}), V denotes the volume of the adsorbate solution added (L), and M denotes the amount of the adsorbent used (g).

2.7 Characterization

2.7.1 SEM Analysis

The morphology of all standard BCs was studied using the SEM coupled with energy-dispersive X-ray spectroscopy (SEM/EDS) analysis technique using a Phenom ProX microscope (Thermo Fisher Scientific, Asheville, USA) at an acceleration voltage of 15 kV. Each of the analyzed samples was previously prepared by individually mounting them onto aluminum stubs using adhesive carbon tape. The substrate was sputter-coated with gold using a BAL-TEC SCD 050 sample coater/sputter (Capovani Brothers Inc., Scotia, USA) to form a thick uniform layer.

2.7.2 FTIR Analysis

The FTIR technique was used for sample analysis using a Bruker, Tensor 27, FTIR Spectrometer (Bruker Corporation, Billerica, Massachusetts, USA). A total of 32 scans were used to analyze the spectral region (320-4000 cm^{-1}) at a resolution of 4 cm^{-1}. This analysis was restricted to the BCs that were selected for the sorption experiments with MB. The aim was to shed some light on the adsorption mechanism(s) involved. The pressed translucent pellets were prepared using 1:50 mg powdered BC and dry KSCN/KBr (0.2%).

2.8 Kinetic Modelling

Batch sorption experiments were performed to determine the effect of the contact time. The vials containing the MB solution (50 mg L^{-1}) and the BC samples were stirred (130 rpm) at a controlled temperature (25°C). BC (0.1 g) was suspended in an aqueous solution of MB (10 mL), and it was kept in contact in an orbital shaker incubator (BT 400, Biothec, Brazil) during different time intervals (0, 5, 15, 60, 120, 240, 360, and 480 min). After each run, the BC sample was removed under conditions of centrifugation at 6,000 rpm (time: 15 min), and the MB concentration in the remaining solution was determined using the UV-vis technique. The experiments were carried out in duplicate.

The kinetic adsorption modeling method was used to mathematically describe the adsorption of MB onto the selected BCs. Non-linear kinetic models of pseudo-first-order (PFO) [43, 44] and pseudo-second-order (PSO) [45, 46] were used for analysis. The non-linear kinetic expressions for the PFO and the PSO models are determined using Eq. (3) and Eq. (4), respectively, as follows:

$$q_t = q_e.\left(1 - exp^{(-k_1 t)}\right), \tag{3}$$

$$q_t = \frac{k_2 . q_e^2 \ t}{1 + \ k_2 . q_e . t}, \tag{4}$$

where t is the contact time (min), q_t is the amount of the adsorbate adsorbed at a time (mg g^{-1}), q_e is the equilibrium adsorption capacity (mg g^{-1}), k_1 is the pseudo-first-order rate constant (min^{-1}), and k_2 is the pseudo-second-order rate constant (g mg^{-1} min^{-1}).

3. Results and Discussion

3.1 MB Calibration Curve

The MB calibration curve was generated by plotting the absorbance recorded using the UV-vis spectrophotometer versus the concentration of each calibration standard (Figure S2). The analytical curve equation is as follows:

$$y = 0.12104x + 0.01356 \quad (5)$$

The adjusted correlation coefficient ($R^2_{ajd.}$) was 0.99747, which is close to unity. The results showed satisfactory linearity in the range of the study.

3.2 pH at the PZC

The difference between pH_i and pH_f (ΔpH) was plotted against the pH_i values, and the pH at PZC (pH_{PZC}) corresponded to the point of intersection in the resulting curve (Figure 1A and Figure 1B). The pH_{PZC} values recorded in a solution of $NaNO_3$ (0.1 mol L^{-1}) are presented in Table S2.

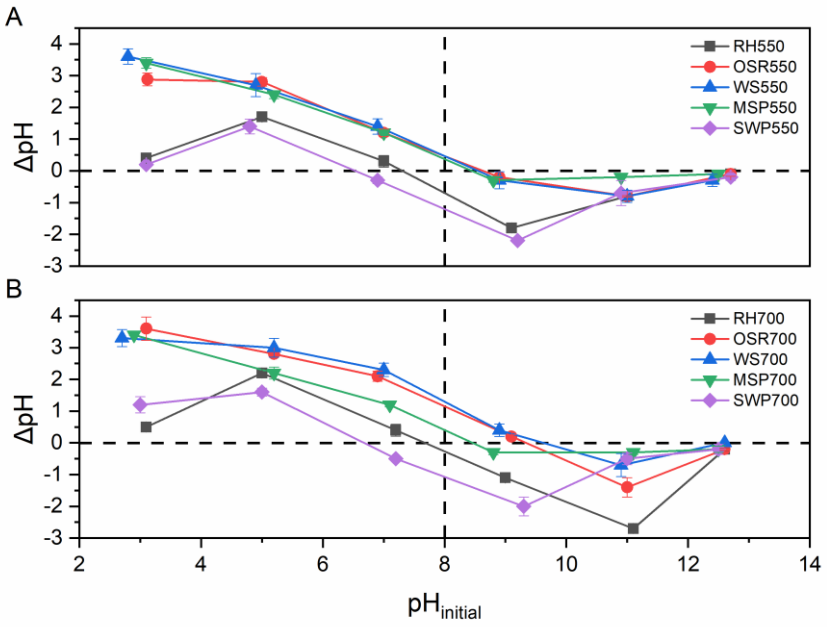

Figure 1 pH at PZC for the BCs (A) pyrolyzed at 550°C and (B) 700°C. Data are expressed as mean ±standard deviations.

The BCs that presented the lowest PZC values were compatible with cationic dyes, such as MB, because the pH of the solution could be easily adjusted to be higher than the pH at PZC. When pH > pH_{PZC}, the surface of the BC remains negatively charged. This favors the adsorption of cations.

Therefore, the most suitable BCs for which it was easy to tune the pH of the solution above pH at PZC were RH550 (PZC = 7.22), RH700 (PZC = 7.64), SWP550 (PZC = 6.57), and SWP700 (PZC = 6.78).

On the other hand, the BCs characterized by high PZC values can be used for the adsorption of anionic dyes as the surfaces of the BCs were positively charged when the pH of the solutions was less than the PZC values of the BCs.

A slight increase in the pH at the PZC values was observed for all BCs obtained at high pyrolytic temperatures (700°C). This could be attributed to the release of alkaline salts, such as Na, K, Ca, and Mg, from the feedstock during the pyrolysis process [47, 48]. This is consistent with previous findings presented in the literature. It has been previously reported that most of the BCs produced following the slow pyrolysis process are alkaline [49-55]. A comparison of the pH_{PZC} values of different BCs reported in the literature is presented in Table S3.

3.3 Adsorption of MB

Based on the PZC results, four BCs (SWP550, SWP700, RH550, and RH770) were selected for further tests to determine the MB adsorption ability. Initially, the adsorption was carried out on the BC samples, and the method was followed by a separation process using paper filters. The combined effect on the removal of MB is presented in Figure 2.

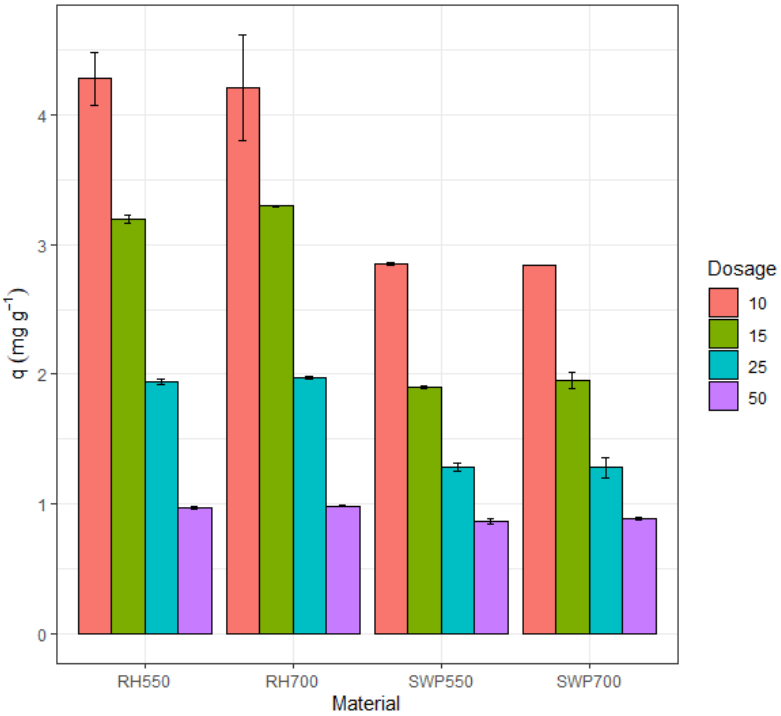

Figure 2 Adsorption capacity q (mg g^{-1}) of BC combined with the filter over a dosage range of 10-50 g L^{-1}. RH and SWP were prepared at 550°C and 700°C. Conditions: MB concentration: 50 mg L^{-1}, contact time: 24 h, temperature 25 ± 2°C. Initial pH = 8.

The maximum values of q (mg g^{-1}) were obtained at the lowest dosage (10 g L^{-1}). Better removal was achieved when higher dosages were used (Figure S2). Further experiments were conducted at this dosage value as the initial aim was to increase the adsorption capacity (10 g L^{-1}). In these experiments, the combined effects of the BC and the filter on the MB removal efficiency were

considered. Firstly, the BC and solutions were separated using the process of centrifugation. The method was also carried out using paper filters. The adsorption capacity and MB removal efficiency of SWP550, SWP700, RH550, and RH770 under the condition of centrifugation and filtration are shown in Figure 3.

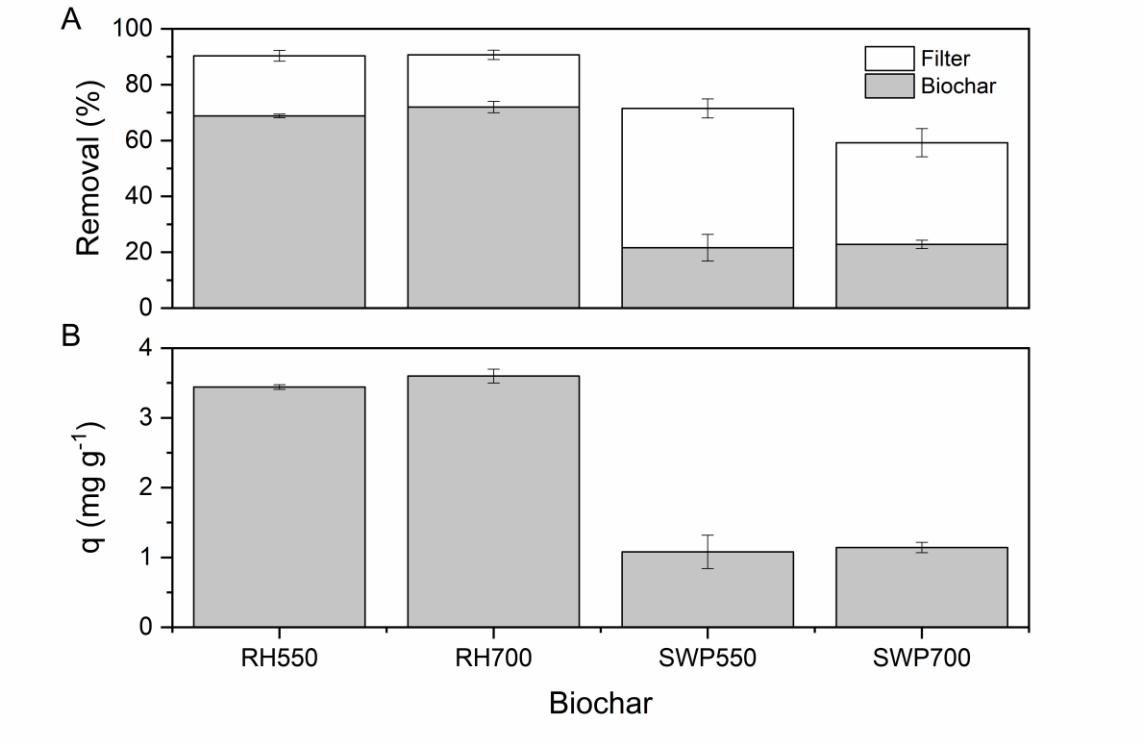

Figure 3 (A) MB removal efficiency of BCs (grey fill) and filter units (white fill); (B) Adsorption capacity q (mg g^{-1}) of the BCs. RH and SWP were prepared at 550°C and 700°C. Conditions: adsorbent dose: 10 g L^{-1}, MB concentration: 50 mg L^{-1}, contact time: 24 h, temperature: 25 ± 2°C. Initial pH = 8.

When only BC was used (i.e., the centrifugation conditions were used for adsorption), an average removal rate of 70% was achieved for both RH BCs (68.83% for RH550 and 71.97% for RH700). The MB removal efficiencies for SWP550 and SWP700 were 21.61% and 22.84%, respectively.

These results indicate that RH BCs present a higher density of negative surface charges compared to SWP BCs. The results agree well with the results obtained by analyzing the pH at PZC (given that the pH of the MB solution was adjusted to a value that was higher than this parameter ($pH = 8 > pH_{PZC}$)). As MB is a cationic dye, its adsorption was realized by exploiting the electrostatic attraction generated on the surface of the RH BC. According to Ahmad et al. [56], the electrostatic affinity between the surface of the BC and the cationic molecules in the MB dye promote the process of adsorption.

The results are consistent with the results reported in the literature. A variety of BCs obtained by pyrolyzing the *Wodyetia bifurcata* endocarp was evaluated as an alternative adsorbent for MB [57]. The authors reported a 60% MB removal rate, regardless of the particle sizes used in the tests (<0.234 nm; 0.234 - 0.300 nm). The adsorption capacity (q_{exp}) of the *Wodyetia bifurcata*-

based biochar ($C_{0[MB]}$: 50 mg L^{-1}, pyrolysis temperature: 700°C, average particle diameter: <0.234 nm, chemically activated with H_3PO_4) was 1.55 mg g^{-1}. It was slightly higher than the adsorption capacity recorded for SWP550 (1.08 mg g^{-1}) and SWP700 (1.14 mg g^{-1}). However, it was significantly lower than the adsorption capacities recorded for RH550 (3.44 mg g^{-1}) and RH700 (3.60 mg g^{-1}).

Hoslett et al. [58] investigated the BC prepared by pyrolyzing the mixed municipal discarded material (MMDM) for the removal of MB. Under some pyrolysis conditions/biochar compositions, the authors reported 2.96 mg g^{-1} as the amount of MB adsorbed. The initial MB concentration was the same as the initial concentration reported herein ($C_{0[MB]}$ = 50 mg L^{-1}).

In another reported study [56], RH biochar, prepared at 500°C under conditions of pyrolysis, was used for the removal of MB from aqueous solutions. The removal percentage reported was in the range of 71.0-99.0%. The removal percentages depended on the experimental conditions. The high adsorption capacity achieved using the RH biochar can be attributed to the different experimental conditions and/or mixture time, which ranged between 0.0 to 96.0 h.

It is worth mentioning that although the performances of SWP550 and SWP700 were poorer compared to the performances of RH550 and RH700, the MB adsorption capacity can be improved by tuning other experimental conditions.

Moreover, no significant difference was observed between the BCs produced from the same biomass but at different temperatures. This indicated that the adsorption of MB was purely dependent on the surface charge and not on physical properties (such as specific surface area). It also revealed that the adsorption process was dominated by the properties of the biomass used.

The positive effect of the filter was also evident in all cases (Figure 2A). When the adsorption process was combined with the filtration process, an increase in the removal percentage of MB (from 20% to >50%) was observed for the SWP BCs. Similarly, the removal percentages recorded using the RH BCs reached approximately 90% MB when both biochar and filter were used for MB removal. This reveals that the combined treatment methods can be used for MB removal, and the results reveal that various waste-derived BCs can be used for MB removal.

The final pH was varied depending on the biosorbent used (Figure S3). For the RH BCs, the final pH values remained above the respective PZC values. Low levels of interferences were observed during the adsorption process. However, the final pH values for the SWP BCs were noticeably affected, and these values approached the PZC values, indicating that the initial adjustment of the pH of the MB solution to 8 did not suffice to uphold the negative charges at the surfaces of the BCs throughout the adsorption process. Therefore, the low removal efficiency was realized for these materials when the adsorption was carried out under the described conditions, indicating that SWP BCs could display a better performance if the pH of the solution was adjusted to a higher value.

3.4 Characterization

3.4.1 Morphological Analysis of the Standard BCs using the SEM Technique

The SEM images of all standard BCs produced at 550°C, and 700°C are shown in Figure 4.

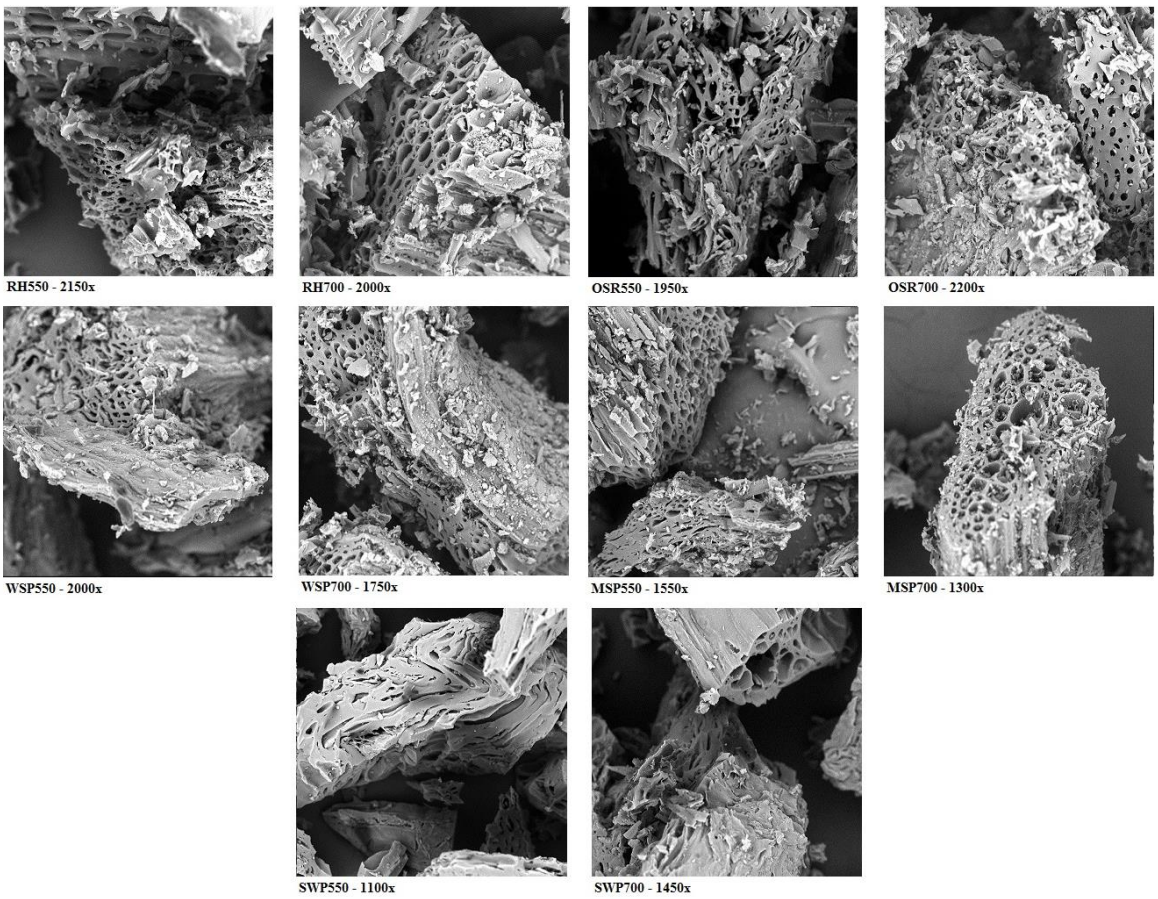

Figure 4 Micrographs of standard BCs.

The topographic images are characteristic of chars. A comparison of the SEM images of RH, WSP, OSR, and MSP reveals that the pyrolytic temperature gap between the BCs obtained at 550°C and those obtained at 700°C were not large enough to create a significant difference in the morphology of the materials. The morphologies could be compared as a similar pyrolytic process was followed for all samples. Pores of different sizes were observed in both sets of samples. This can be potentially attributed to the dehydration and volatilization of the biomasses [59].

The pattern recorded for the SWP BCs was different from the patterns recorded for other biochars. The presence of irregular longitudinal structures remnant of the fibrous cellulosic composition of softwood was observed. In this case, however, an increase in the pyrolytic temperature appeared to have changed the morphology of the sample. Larger pores are observed in the SWP700 sample, which is consistent with the findings of Maziarka et al. [60]. They reported that the specific surface area (SSA) and pore volume increased with an increase in the pyrolytic temperature. Similar observations were made for other BCs, but the difference in the pore size could not be visually detected by analyzing the SEM images.

3.4.2 FTIR-based Surface Analysis

The superposition of the FTIR spectral profiles corresponding to the RH and the SWP BCs, recorded before and after MB adsorption, are presented in Figure 5. The results showed that the difference in the pyrolytic temperature at which the BC samples were obtained exerted a subtle

influence on the surface functional groups of the BCs. In the profiles recorded for the RH700 and the SWP700 samples, the peaks observed for RH550 and SWP550 were present. However, these peaks were slightly less intense. The results agree well with the results obtained during the thermal degradation process [48, 61, 62].

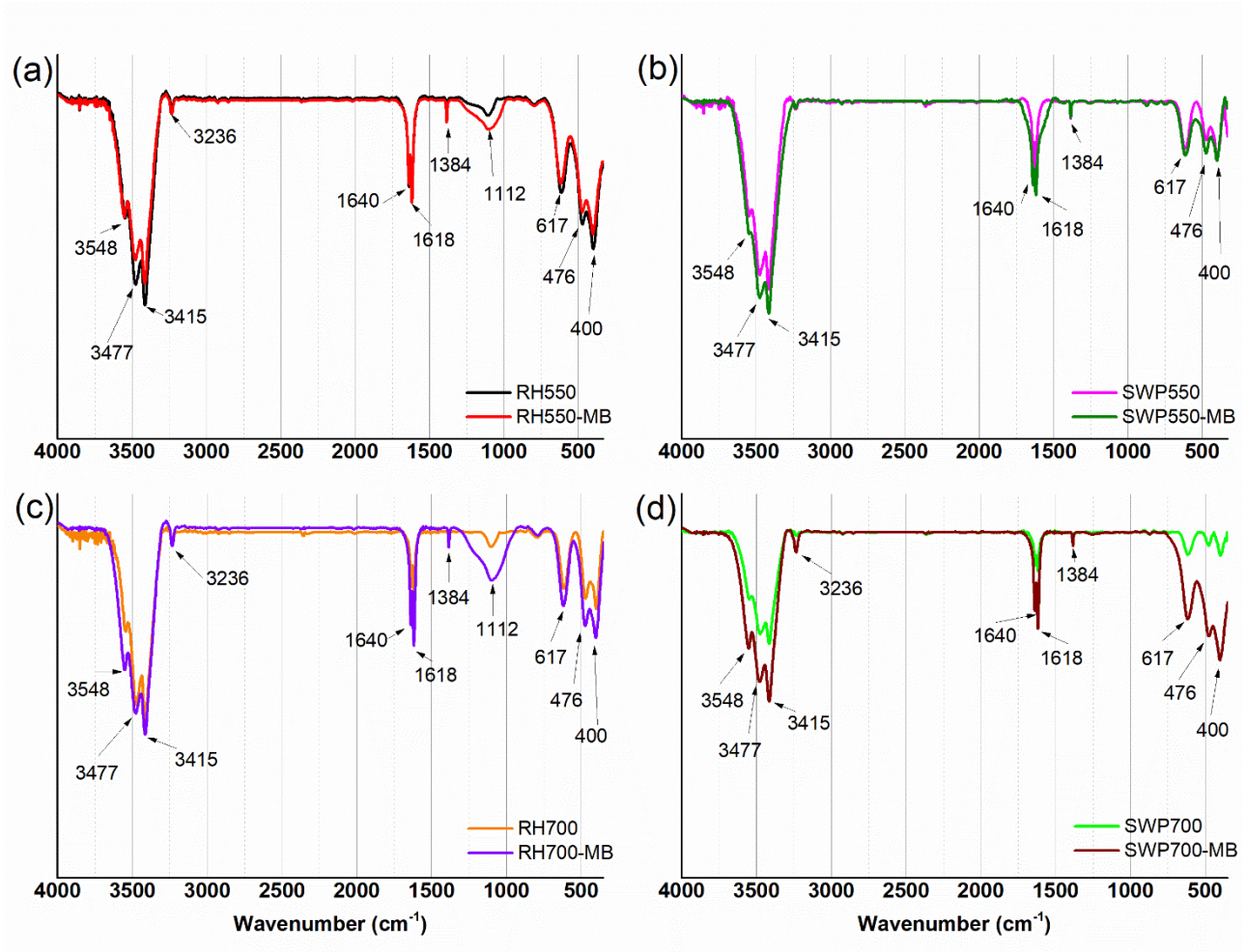

Figure 5 FTIR spectral profiles recorded for (a) RH550, (b) SWP550, (c) RH700, and (d) SWP700.

The spectral profiles recorded for RH (Figure 5(a) and Figure 5(c)) were analyzed. The peaks in the region between 3600 and 3100 cm^{-1} are commonly attributed to the characteristic stretching vibrations of the -OH group in Si-OH (silanol) or water. The absorption peaks at 1640 cm^{-1} and 1618 cm^{-1} were assigned to the C=O group of carboxyl and carbonyl groups [63]. The peak at 1384 cm^{-1} was attributed to the C=C stretching vibration, consistent with the aromatic groups in lignin [64]. The peak at 1112 cm^{-1} is indicative of the presence of the Si-O-Si group [65], and the peak at 617 cm^{-1} can be attributed to the Si-OH group [66]. This can be explained by the fact that rice husk contains a high content of silica [67]. The characteristic peaks obtained for each raw RH BC are also present in the FTIR spectral profiles of both BCs post MB adsorption. However, these peaks are more intense.

The presence of several peaks attributable to the RH BCs was observed in the spectral profile recorded for SWP. However, the peak associated with the siloxane bonds (Si-O-Si) between 1000

cm^{-1} and 1300 cm^{-1} was absent in the profile recorded for SWP. The absorption intensities of the bands at 1640 cm^{-1}, 1618 cm^{-1}, and 3430 cm^{-1} increased after MB adsorption.

3.5 Kinetic Study

The efficiency and the equilibrium adsorption capacity of the RH BCs were evaluated by conducting an adsorption kinetic study. The RH BCs were selected based on their adsorption performance. The results indicated that they were potential adsorbent materials for MB in aqueous solutions. The effect of the contact time on the removal of MB by RH BC is shown in Figure 6. A minimum of 1 h was necessary to reach the adsorption equilibrium, at which the equilibrium capacities, according to the non-linear pseudo-second-order model, were 2.88 mg g^{-1} and 2.97 mg g^{-1} for RH550 and RH700, respectively. These results were similar to the results reported by Gülen et al. [68]. They used sumac leaves for MB adsorption and reported that the adsorption capacity was in the range of 0.85-3.20 mg g^{-1}. This range was a result of various initial MB concentrations, as assessed by the authors. Adsorption equilibrium was reached at 30 min. A high adsorption capacity for MB was achieved using carbonized chestnut shells (5.13 mg g^{-1}). However, the equilibrium was reached at 120 min [69].

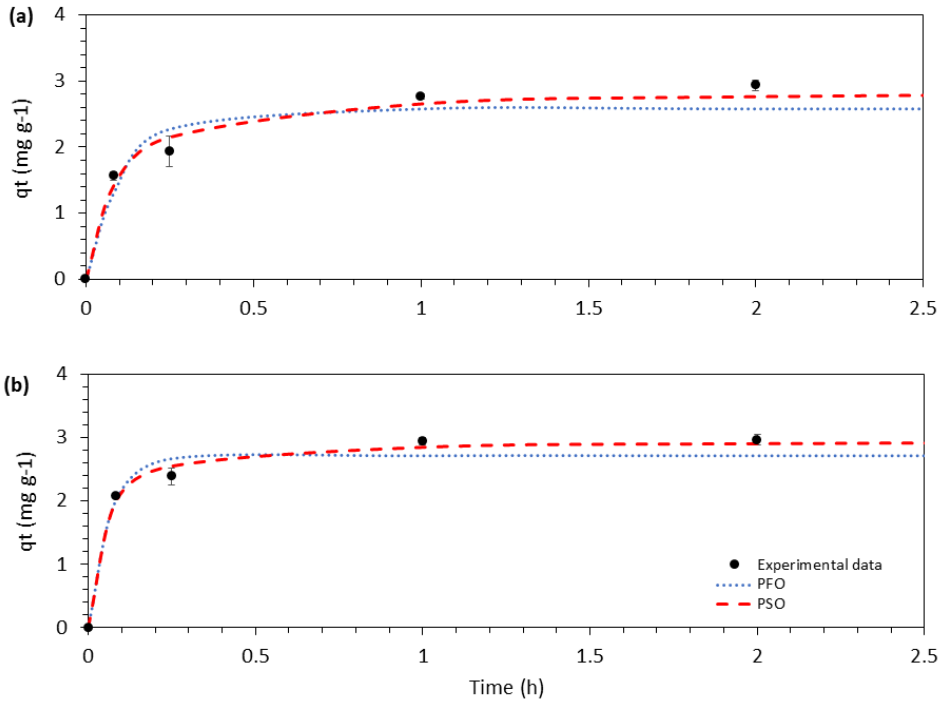

Figure 6 Experimental kinetics for the removal of MB from an aqueous solution using (a) RH550 and (b) RH700. (●) Experimental data; (dotted blue line) data predicted using the pseudo-first-order model; (dashed red line) data predicted using the pseudo-second-order model.

The linear kinetic parameters of each model are presented in Table 2. According to the data, the PSO model presented a better fit, with the R^2 values being close to 1 for the RH BCs (0.9759 for RH550 and 0.9799 for RH700).

Table 2 Kinetic parameters corresponding to pseudo-first-order and pseudo-second-order models for the adsorption of MB onto RH550 and RH700. Values of $q_{e,exp}$ for RH550 and RH700 were recorded after 1 h.

Adsorbent	$q_{e\ exp}$ (mg g^{-1})	PFO k_1 (h^{-1})	PFO q_e (mg g^{-1})	PFO R^2	PSO k_2 (g mg^{-1} h^{-1})	PSO q_e (mg g^{-1})	PSO R^2
RH550	2.76	8.53	2.59	0.9327	4.09	2.88	0.9759
RH700	2.95	16.25	2.71	0.9348	8.32	2.97	0.9799

The calculated equilibrium sorption capacities (q_e) for the PSO model were closer to the experimental results ($q_{e\ exp}$), suggesting that the sorption of MB onto the RH BCs followed the PSO model. In other words, more than one step is likely involved in the sorption process. The PSO model was also the best fit for the MB adsorption process conducted using sumac leaves [68], carbonized chestnut shell [69], and carbonized peanut shell [70]. The values of the kinetic parameters k_1 and k_2 corroborate the results obtained during the ultrasonic-assisted adsorption of MB in the presence of sumac leaves [68].

Finally, the pH values of the solutions were measured at the same time intervals of the kinetic study (Figure S4). At the equilibrium corresponding to RH550 and RH700, the pH values remained higher than the respective PZC values (9.4 and 9.6, respectively). The results revealed that these contact times could be successfully used to perform the adsorption of MB from aqueous solutions.

4. Conclusions

The results revealed the considerable differences in the PZC values of the ten BC samples under study. This information was then used for the selection of BC samples to match the requirements of cationic dye (MB) removal from wastewater and drinking water. Under the given conditions, RH BCs performed the best as MB adsorbent materials, indicating that these BCs presented were characterized by the presence of a large number of negative charges. The quantity of negative charge, in this case, was higher than that recorded for the SWP BCs. When RH and SWP BCs were produced under similar pyrolytic conditions, it was expected that they would exhibit different adsorbent properties, as the characteristics of each BC depended significantly on the feedstock source. Moreover, SWP BCs are likely to perform better under optimized experimental conditions. An in-depth experimental investigation should be conducted to validate this hypothesis. The equilibrium was reached after 4 h and 6 h for RH550 and RH700, respectively, and the adsorption process was best represented by the pseudo-second-order rate model. The performances of the RH and SWP BCs can be improved in the future by optimizing the adsorption parameters and activating these BCs.

Acknowledgments

The authors would like to acknowledge the Brazilian National Nuclear Energy Commission (CNEN-SP) for supporting this study and the Biochar Research Centre (UKBRC, University of Edinburgh, UK) for supplying the standard biochars.

Author Contributions

Conceptualization: [SNG], [OM], [LGA]; Data curation: [SNG], [TW], [TTS], [SR], [LGA]; Formal analysis: [SNG], [TW], [LGA]; Funding acquisition: [SNG], [JTM], [JAST], [OM]; Investigation: [SNG], [TW], [TTS], [SR], [LGA]; Methodology: [SNG], [LGA]; Project administration: [SNG], [LGA]; Resources: [JTM], [JAST], [OM]; Validation: [TW]; Writing - original draft preparation: [SNG], [LGA]; Writing - review and editing: [SNG], [JTM], [OM], [LGA]; Funding acquisition: [SNG], [JTM], [JAST], [OM]; Resources: [JTM], [JAST], [OM]; Supervision: [JTM], [JAST], [OM], [LGA].

Funding

This research was funded by the National Nuclear Energy Commission (CNEN-SP, Brazil).

Competing Interests

The authors have declared that no competing interests exist.

Additional Materials

The following additional materials are uploaded at the page of this paper.

1. Table S1: UKBRC specification sheets containing the detailed properties of the ten standard biochars used in this study [71].
2. Figure S1: UKBRC standard biochars and their feedstocks [72].
3. Table S2: PZC values obtained for the ten standard biochars.
4. Table S3: Comparison of pH_{PZC} values of different biochars. * NPB and BPB refer to newspaper biochar and book paper biochar, respectively.
5. Figure S2: Removal efficiency of MB by biochars combined with the filter over a dosage range of 10-50 g L^{-1}. RH and SWP were prepared at 550°C and 700°C. Conditions: MB concentration: 50 mg L^{-1}, contact time: 24 h, temperature: 25 ± 2°C. Initial pH = 8.
6. Figure S3: pH after 24h as a result of the mixture between MB and the RH and SWP biochars prepared at 550°C and 700°C. Conditions: adsorbent dose: 10 g L^{-1}, MB concentration: 50 mg L^{-1}, contact time: 24 h, 25 ± 2°C. Initial pH = 8 for all conditions.
7. Figure S4: pH values measured at the same time intervals of the kinetic study for MB's adsorption process by RH550 (a) and RH700 (b). Conditions: adsorbent dose: 10 g L^{-1}, MB concentration: 50 mg L^{-1}, contact times: 0, 5, 15, 60, 120, 240, 360, and 480 min, 25 ± 2°C. Initial pH = 8 for all conditions.

References

1. Lellis B, Fávaro Polonio CZ, Pamphile JA, Polonio JC. Effects of textile dyes on health and the environment and bioremediation potential of living organisms. Biotechnol Res Innov. 2019; 3: 275-290.
2. Padhi BS. Pollution due to synthetic dyes toxicity & carcinogenicity studies and remediation. Int J Environ Sci. 2012; 3: 940-955.

3. Chequer FMD, De Oliveira GAR, Ferraz ERA, Cardoso JC, Zanoni MVB, De Oliveira DP. Textile dyes: Dyeing process and environmental impact. Eco-Friendly Text Dye Finish. 2013; 6: 151-176.
4. Stolz A. Basic and applied aspects in the microbial degradation of azo dyes. Appl Microbiol Biotechnol. 2001; 56: 69-80.
5. Manu B, Chaudhari S. Decolorization of indigo and azo dyes in semicontinuous reactors with long hydraulic retention time. Process Biochem. 2003; 38: 1213-1221.
6. Wang H, Yuan X, Zeng G, Leng L, Peng X, Liao K, et al. Removal of malachite green dye from wastewater by different organic acid-modified natural adsorbent: Kinetics, equilibriums, mechanisms, practical application, and disposal of dye-loaded adsorbent. Environ Sci Pollut Res. 2014; 21: 11552-11564.
7. Samsami S, Mohamadizaniani M, Sarrafzadeh MH, Rene ER, Firoozbahr M. Recent advances in the treatment of dye-containing wastewater from textile industries: Overview and perspectives. Process Saf Environ Prot. 2020; 143: 138-163.
8. Islam MR, Mostafa MG. Textile dyeing effluents and environment concerns-a review. J Environ Sci Nat Resour. 2018; 11: 131-144.
9. Kant R. Textile dyeing industry an environmental hazard. Nat Sc. 2012; 4: 22-26.
10. Benkhaya S, M'rabet S, El Harfi A. A review on classifications, recent synthesis and applications of textile dyes. Inorg Chem Commun. 2020; 115:107891.
11. Ghasemi J, Asadpour S. Thermodynamics' study of the adsorption process of methylene blue on activated carbon at different ionic strengths. J Chem Thermodyn. 2007; 39: 967-971.
12. Eren E. Investigation of a basic dye removal from aqueous solution onto chemically modified Unye bentonite. J Hazard Mater. 2009; 166: 88-93.
13. Crini G. Recent developments in polysaccharide-based materials used as adsorbents in wastewater treatment. Prog Polym Sci. 2005; 30: 38-70.
14. Vargas AMM, Cazetta AL, Kunita MH, Silva TL, Almeida VC. Adsorption of methylene blue on activated carbon produced from flamboyant pods (*Delonix regia*): Study of adsorption isotherms and kinetic models. Chem Eng J. 2011; 168: 722-730.
15. Rehman MSU, Kim I, Han JI. Adsorption of methylene blue dye from aqueous solution by sugar extracted spent rice biomass. Carbohydr Polym. 2012; 90: 1314-1322.
16. Toor M, Jin B. Adsorption characteristics, isotherm, kinetics, and diffusion of modified natural bentonite for removing diazo dye. Chem Eng J. 2012; 187: 79-88.
17. Azari A, Nabizadeh R, Nasseri S, Mahvi AH, Mesdaghinia AR. Comprehensive systematic review and meta-analysis of dyes adsorption by carbon-based adsorbent materials: Classification and analysis of last decade studies. Chemosphere. 2020; 250: 126238.
18. Ghaedi M, Larki HA, Kokhdan SN, Marahel F, Sahraei R, Daneshfar A, Purkait MK. Synthesis and characterization of zinc sulfide nanoparticles loaded on activated carbon for the removal of methylene blue. Environ Prog Sustain Energy. 2013; 32: 535-542.
19. Liu Y, Kang Y, Mu B, Wang A. Attapulgite/bentonite interactions for methylene blue adsorption characteristics from aqueous solution. Chem Eng J. 2014; 237: 403-410.
20. Roosta M, Ghaedi M, Daneshfar A, Sahraei R, Asghari A. Optimization of the ultrasonic assisted removal of methylene blue by gold nanoparticles loaded on activated carbon using experimental design methodology. Ultrason Sonochem. 2014; 21: 242-252.

21. Roosta M, Ghaedi M, Daneshfar A, Sahraei R. Experimental design based response surface methodology optimization of ultrasonic assisted adsorption of safaranin O by tin sulfide nanoparticle loaded on activated carbon. Spectrochim. Acta Part A Mol Biomol Spectrosc. 2014; 122: 223-231.
22. Zhang X, Wang H, He L, Lu K, Sarmah A, Li J, et al. Using biochar for remediation of soils contaminated with heavy metals and organic pollutants. Environ Sci Pollut Res. 2013; 20: 8472-8483.
23. Mohan D, Sarswat A, Ok YS, Pittman Jr CU. Organic and inorganic contaminants removal from water with biochar, a renewable, low cost and sustainable adsorbent–A critical review. Bioresour Technol. 2014; 160: 191-202.
24. Parshetti GK, Chowdhury S, Balasubramanian R. Hydrothermal conversion of urban food waste to chars for removal of textile dyes from contaminated waters. Bioresour Technol. 2014; 161: 310-319.
25. Gurav R, Bhatia SK, Choi TR, Choi YK, Kim HJ, Song HS, et al. Application of macroalgal biomass derived biochar and bioelectrochemical system with Shewanella for the adsorptive removal and biodegradation of toxic azo dye. Chemosphere. 2021; 264: 128539.
26. Iqbal J, Shah NS, Sayed M, Niazi NK, Imran M, Khan JA, et al. Nano-zerovalent manganese/biochar composite for the adsorptive and oxidative removal of Congo-red dye from aqueous solutions. J Hazard Mater. 2021; 403: 123854.
27. Yu KL, Lee XJ, Ong HC, Chen WH, Chang JS, Chang JS, et al. Adsorptive removal of cationic methylene blue and anionic Congo red dyes using wet-torrefied microalgal biochar: Equilibrium, kinetic and mechanism modeling. Environ Pollut. 2021; 272: 115986.
28. Sohi SP, Krull E, Lopez Capel E, Bol R. A review of biochar and its use and function in soil. Adv Agron. 2010; 105: 47-82.
29. Giacomni F, Benedet Menegazzo MA, da Silva MG, da Silva AB, Simoes Dornellas de Barros MA. Point of zero charge of protein fibers, an important characteristic for dyeing. Matéria. 2017; 22. doi: 10.1590/S1517-707620170002.0159.
30. Stumm W, Morgan JJ. Aquatic chemistry: Chemical equilibria and rates in natural waters. New York: John Wiley Sons; 2012.
31. Sposito G. The chemistry of soils. Oxford: University of Oxford; 2008.
32. Chen Z, Chen B, Zhou D, Chen W. Bisolute sorption and thermodynamic behavior of organic pollutants to biomass-derived biochars at two pyrolytic temperatures. Environ Sci Technol. 2012; 46: 12476-12483.
33. Sun J, Lian F, Liu Z, Zhu L, Song Z. Biochars derived from various crop straws: Characterization and Cd (II) removal potential. Ecotoxicol Environ Saf. 2014; 106: 226-231.
34. Cao X, Ma L, Gao B, Harris W. Dairy-manure derived biochar effectively sorbs lead and atrazine. Environ Sci Technol. 2009; 43: 3285-3291.
35. Xu X, Cao X, Zhao L. Comparison of rice husk-and dairy manure-derived biochars for simultaneously removing heavy metals from aqueous solutions: Role of mineral components in biochars. Chemosphere. 2013; 92: 955-961.
36. Xu X, Cao X, Zhao L, Wang H, Yu H, Gao B. Removal of Cu, Zn, and Cd from aqueous solutions by the dairy manure-derived biochar. Environ Sci Pollut Res. 2013; 20: 358-368.
37. Pathania D, Sharma S, Singh P. Removal of methylene blue by adsorption onto activated carbon developed from *Ficus carica* bast. Arab J Chem. 2017; 10: S1445-S1451.

38. Satilmis B, Budd PM. Selective dye adsorption by chemically-modified and thermally-treated polymers of intrinsic microporosity. J Colloid Interface Sci. 2017; 492: 81-91.
39. Hurairah SN, Lajis NM, Halim AA. Methylene blue removal from aqueous solution by adsorption on *Archidendron jiringa* seed shells. J Geosci Environ Prot. 2020; 8: 128-143.
40. Dong Y, Lu B, Zang S, Zhao J, Wang X, Cai Q. Removal of methylene blue from coloured effluents by adsorption onto SBA-15. J Chem Technol Biotechnol. 2011; 86: 616-619.
41. Han Q, Wang J, Goodman BA, Xie J, Liu Z. High adsorption of methylene blue by activated carbon prepared from phosphoric acid treated eucalyptus residue. Powder Technol. 2020; 366: 239-248.
42. Guo JZ, Li B, Liu L, Lv K. Removal of methylene blue from aqueous solutions by chemically modified bamboo. Chemosphere. 2014; 111: 225-231.
43. Lagergren S. Zur theorie der sogenannten adsorption gelöster stoffe. Kungliga Svenska Vetenskapsakademiens. Handlingar. 1898; 24: 1-39.
44. Ho YS, McKay G. A comparison of chemisorption kinetic models applied to pollutant removal on various sorbents. Process Saf Environ Prot. 1998; 76: 332-340.
45. Blanchard G, Maunaye M, Martin G. Removal of heavy metals from waters by means of natural zeolites. Water Res. 1984; 18: 1501-1507.
46. Lima L, Bento C, Silva M, Vieira M. Fixed bed biosorption using aquatic macrophyte in lead removal. Blucher Chem Eng Proc. 2015; 1: 6425-6432.
47. Ahmad M, Lee SS, Dou X, Mohan D, Sung JK, Yang JE, et al. Effects of pyrolysis temperature on soybean stover-and peanut shell-derived biochar properties and TCE adsorption in water. Bioresour Technol. 2012; 118: 536-544.
48. Kim WK, Shim T, Kim YS, Hyun S, Ryu C, Park YK, et al. Characterization of cadmium removal from aqueous solution by biochar produced from a giant *Miscanthus* at different pyrolytic temperatures. Bioresour Technol. 2013; 138: 266-270.
49. Liu Y, Zhao X, Li J, Ma D, Han R. Characterization of bio-char from pyrolysis of wheat straw and its evaluation on methylene blue adsorption. Desalin Water Treat. 2012; 46: 115-123.
50. Jindo K, Mizumoto H, Sawada Y, Sanchez Monedero MA, Sonoki T. Physical and chemical characterization of biochars derived from different agricultural residues. Biogeosciences. 2014; 11: 6613-6621.
51. Tan X, Liu Y, Zeng G, Wang X, Hu X, Gu Y, et al. Application of biochar for the removal of pollutants from aqueous solutions. Chemosphere. 2015; 125: 70-85.
52. Vyavahare G, Jadhav P, Jadhav J, Patil R, Aware C, Patil D, et al. Strategies for crystal violet dye sorption on biochar derived from mango leaves and evaluation of residual dye toxicity. J Clean Prod. 2019; 207: 296-305.
53. Wang F, Zeng Q, Su W, Zhang M, Hou L, Wang ZL. Adsorption of bisphenol A on peanut shell biochars: The effects of surfactants. J Chem. 2019; 2019. doi: 10.1155/2019/2428505.
54. Xu X, Hu X, Ding Z, Gao B. Sorption of aqueous methylene blue, cadmium and lead onto biochars derived from scrap papers. Polish J Environ Stud. 2020; 29: 4409-4423.
55. Zubair M, Mu'azu ND, Jarrah N, Blaisi NI, Aziz HA, A Harthi MA. Adsorption behavior and mechanism of methylene blue, crystal violet, Eriochrome black T, and methyl orange dyes onto biochar-derived date palm fronds waste produced at different pyrolysis conditions. Water Air Soil Pollut. 2020; 231: 1-19.

56. Ahmad A, Khan N, Giri BS, Chowdhary P, Chaturvedi P. Removal of methylene blue dye using rice husk, cow dung and sludge biochar: Characterization, application, and kinetic studies. Bioresour Technol. 2020; 306: 123202.
57. Dos Santos KJL, Dos Santos GES, de SáÍMGL, Ide AH, da Silva Duarte JL, de Carvalho SHV, et al. Wodyetia bifurcata biochar for methylene blue removal from aqueous matrix. Bioresour. Technol. 2019; 293: 122093.
58. Hoslett J, Ghazal H, Mohamad N, Jouhara H. Removal of methylene blue from aqueous solutions by biochar prepared from the pyrolysis of mixed municipal discarded material. Sci Total Environ. 2020; 714: 136832.
59. Bandosz TJ. Activated carbon surfaces in environmental remediation. UK: Elsevier; 2006.
60. Maziarka P, Wurzer C, Arauzo PJ, Dieguez Alonso A, Mašek O, Ronsse F. Do you BET on routine? The reliability of N_2 physisorption for the quantitative assessment of biochar's surface area. Chem Eng J. 2021; 418: 129234.
61. Crombie K, Mašek O. Investigating the potential for a self-sustaining slow pyrolysis system under varying operating conditions. Bioresour Technol. 2014; 162: 148-156.
62. Uchimiya M, Orlov A, Ramakrishnan G, Sistani K. In situ and ex situ spectroscopic monitoring of biochar's surface functional groups. J Anal Appl Pyrolysis. 2013; 102: 53-59.
63. Liu C, Wang W, Wu R, Liu Y, Lin X, Kan H, et al. Preparation of acid-and alkali-modified biochar for removal of methylene blue pigment. ACS Omega. 2020; 5: 30906-30922.
64. Smidt E, Meissl K. The applicability of Fourier transform infrared (FT-IR) spectroscopy in waste management. Waste Manag. 2007; 27: 268-276.
65. Tsai CC, Chang YF. Effects of rice husk biochar on carbon release and nutrient availability in three cultivation age of greenhouse soils. Agronomy. 2020; 10: 990.
66. Nakbanpote W, Goodman BA, Thiravetyan P. Copper adsorption on rice husk derived materials studied by EPR and FTIR. Colloids Surf A Physicochem Eng Asp. 2007; 304: 7-13.
67. De Souza MF, Magalhães WLE, Persegil MC. Silica derived from burned rice hulls. Mater Res. 2002; 5: 467-474.
68. Gülen J, Akın B, Özgür M. Ultrasonic-assisted adsorption of methylene blue on sumac leaves. Desalination Water Treat. 2016; 57: 9286-9295.
69. Gülen J, İskeçeli M. Removal of methylene blue by using porous carbon adsorbent prepared from carbonized chestnut shell. Mater Test. 2017; 59: 188-194.
70. Gülen J, Zorbay F. Methylene blue adsorption on a low cost adsorbent—carbonized peanut shell. Water Environ Res. 2017; 89: 805-816.
71. UK Biochar Research Centre Website. Standard biochar specification sheets for Sewage Sludge, Wheat Straw, Softwood, Rice Husk and Oil Seed Rape Straw biochars [Internet]. Edinburgh: UK Biochar Research Centre Website [cited date 2022 April 17] Available from: https://www.biochar.ac.uk/standard_materials.php.
72. Mašek O, Buss W, Sohi S. Standard biochar materials. Environ Sci Technol. 2018; 52: 9543-9544.

Enjoy *Recent Progress in Materials* by:

1. Submitting a manuscript
2. Joining in volunteer reviewer bank
3. Joining Editorial Board
4. Guest editing a special issue

For more details, please visit:
http://www.lidsen.com/journals/rpm